Oscillatory pairing of fermions in spin-split traps

Kuei Sun, Julia S. Meyer, Daniel E. Sheehy, and Smitha Vishveshwara

Oscillatory pairing of fermions in spin-split traps

Kuei Sun,[1] Julia S. Meyer,[2,3] Daniel E. Sheehy,[4] and Smitha Vishveshwara[1]

[1]*Department of Physics, University of Illinois at Urbana-Champaign, Urbana, IL 61801, USA*
[2]*SPSMS, CEA-INAC/UJF-Grenoble 1, 38054 Grenoble Cedex 9, France*
[3]*Department of Physics, The Ohio State University, Columbus, OH 43210, USA*
[4]*Department of Physics, Louisiana State University, Baton Rouge, LA 70803, USA*

(Dated: January 27, 2011)

As a means of realizing oscillatory pairing between fermions, we study superfluid pairing between two fermion "spin" species that are confined to adjustable spin-dependent trapping potentials. Focusing on the one-dimensional limit, we find that with increasing separation between the spin-dependent traps the fermions exhibit distinct phases, including a fully paired phase, a spin-imbalanced phase with oscillatory pairing, and an unpaired fully spin-polarized phase. We obtain the phase diagram of fermions in such a spin-split trap and discuss signatures of these phases in cold-atom experiments.

PACS numbers: 03.75.Ss, 05.30.Fk, 67.85.Lm, 71.10.Pm

The idea that Cooper pairing in the presence of a density imbalance of two interacting fermion species naturally yields oscillatory pairing correlations in real space was put forth decades ago. However, to date, this phenomenon, known as Fulde-Ferrell-Larkin-Ovchinnikov (FFLO) pairing [1, 2], has not been conclusively observed. (Related effects have been clearly seen in superconductor-ferromagnet hybrid systems where the proximity-induced pair correlations in the ferromagnet exhibit oscillations [3].) In recent years, atomic physics experiments have explored paired fermion superfluidity in cold atomic gases [4–6], a new setting for the observation of FFLO pairing correlations under a density imbalance between the two "spin" species – a possibility that has inspired a large amount of recent theoretical and experimental activity [7]. Much of the excitement follows from the extreme tunability of cold-fermion experiments, which exhibit several experimentally-adjustable parameters including the interactions, the densities of the different species, and the trap geometry. Of late, attention has focused on one-dimensional (1D) systems with global spin imbalance [8–14] or spin-dependent potentials [15, 16], where the parameter regime occupied by the FFLO state is predicted to be significantly wider than in the 3D case [17–19]. Indeed, recent experiments [20] on quasi-1D spin-imbalanced fermionic gases have observed a partially polarized state, although associated oscillatory pairing correlations have yet to be confirmed.

In this Letter, we propose a new 1D setup to achieve FFLO pairing in cold atomic gases: a *balanced* mixture of two hyperfine species of attractively interacting fermionic atoms that are *separately* trapped in a controllable way, as illustrated in Fig. 1(a) – a situation we shall call a "spin-split trap". This setup provides an effective spatially-varying chemical potential difference between the two spin states due to the separate trapping potentials and yields an alternate, dynamically controllable route to achieving oscillatory FFLO-like pair correlations in cold atomic gases, controlled not by an imposed global population imbalance but, rather, by the *separation* between the two traps and the ensuing local imbalance.

The spin-split trap, whose 3D counterpart was studied in Ref. [21], is described by the spin-dependent potentials

$$V_\sigma(z) = \frac{1}{2}m\omega_z^2(z - \sigma d)^2, \tag{1}$$

where ω_z is the trapping frequency, m is the atomic mass and $\sigma = \pm$ correspond to the two hyperfine species. Thus, the centers of the two traps are separated by a distance $2d$. For $d \to 0$, the ground state is a singlet s-wave superfluid with a vanishing spin imbalance everywhere in the cloud. As argued below using local density arguments and a Bogoliubov-de Gennes (BdG) treatment, for nonzero d, however, the split traps promote a local spin imbalance. We find that beyond a critical separation, $d > d_c$, the split-trap geometry displays oscillatory pairing correlations, as depicted in Fig. 1(b), which shows the local pairing amplitude $\Delta(z)$, total density $\rho(z) = \rho_\uparrow(z) + \rho_\downarrow(z)$, and magnetization (spin imbalance) $M(z) = \rho_\uparrow(z) - \rho_\downarrow(z)$.

An intuitive understanding of the spin-split-trap system can be found using the local density approximation (LDA) along with the known behavior of the homogeneous spin-imbalanced gas derived using the Bethe ansatz [9, 10]. The phase diagram, shown in Fig. 2, displays three phases as a function of the net chemical potential $\mu = (\mu_\uparrow + \mu_\downarrow)/2$ versus the chemical potential imbalance (magnetic field) $h = (\mu_\uparrow - \mu_\downarrow)/2$, namely a fully paired (FP) state, a fully polarized (FPo) state, and a partially polarized (PP) state. The PP state is expected to be of the FFLO type, having an oscillatory pairing amplitude [8, 13], as corroborated by our studies below.

Within LDA, the trapping potential in our system enters as a spin-dependent spatially-varying chemical potential, $\mu_\sigma(z) = \mu_0 - V_\sigma(z)$, where μ_0 is the global chemical potential of the system. For the harmonic trap of Eq. (1), μ and
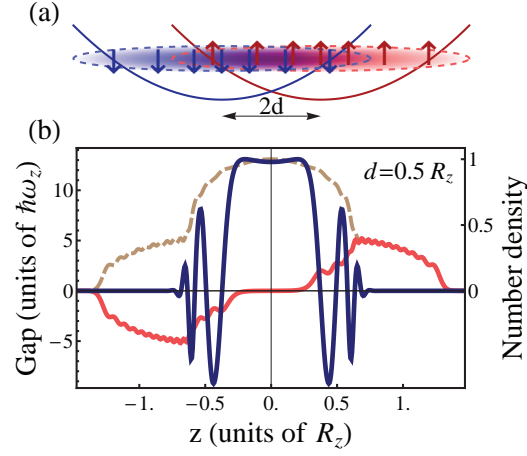
FIG. 1: (Color Online) (a) Illustration of our proposed spin-split trap setup showing separate trapping potentials for two fermion species, ↑ and ↓. (b) Numerically-determined spatial profile of the pairing gap $\Delta(z)$ (solid blue curve, axis on left-hand side of graph), total density $\rho(z)$, and spin imbalance $M(z)$ (dashed light-brown and solid red curves, respectively, axis on right-hand side of graph, normalized by $\max_z[\rho]$), showing oscillatory pairing along with a local imbalance.
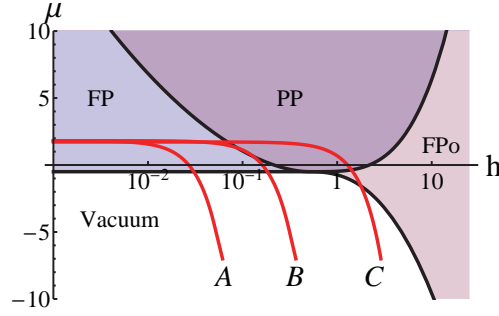

FIG. 2: (Color Online) The local properties of the system in the spin-split trap can be understood using the phase diagram of the uniform imbalanced system, taken from Ref. [9], showing a fully paired (FP), partially polarized (PP), and fully polarized (FPo) phase as well as the vacuum. (Here μ and h are measured in units of $mg^2/4\hbar^2$, where g is the 1D coupling constant.) The red curves A, B, and C represent the LDA trajectories followed as a function of z by the spin-split system for $d < d_c$, $d = d_c$ and $d > d_c$, respectively.

h are then related through $\mu = \mu_0 - h^2/(2m\omega_z^2 d^2)$, which corresponds to downward facing parabolas in the μ versus h phase diagram. In Fig. 2, we show three curves corresponding to different values of the separation d. One can see that they traverse different phases from the center $z = 0$ (where $h = 0$) to the edges of the trap. For small separation d, the system is described by a tight parabola and is thus confined to the fully paired phase. But with increasing d, the parabola broadens and, beyond a critical separation d_c, traverses all three phases as a function of position. In this case, at small z, the local potential imbalance h remains small enough that the system is (locally) fully paired. At larger z, the local h exceeds a critical value such that (locally) the system enters the PP phase. At even larger z, near the edges of the trap, the system is (locally) in a fully polarized normal phase. Thus, the system concurrently hosts all three phases. Note that, in contrast, in the case of a globally spin-imbalanced system with a single trap, the system traces a vertical line in the phase diagram, yielding two regions – a partially polarized core and either fully polarized or fully paired edges [9].

We now model the spin-split system using a microscopic description which enables a more detailed analysis, confirms the salient features described above, and shows a direct correspondence between local spin imbalance and oscillatory pairing. We study two species of fermions, $\hat{\psi}_{\uparrow,\downarrow}(z)$, in a 1D harmonic potential characterized by the trapping frequency ω_z. In atomic systems, this limit can be achieved in a highly anisotropic trap with a transverse trapping frequency ω_r such that $N\omega_z/\omega_r < 1$ and $N|a_s|/R_z \ll 1$ [4, 22]. Here, N is the number of fermions of each spin species, $R_z = \sqrt{2N-1}\,\ell_z$ (with $\ell_z = \sqrt{\hbar/m\omega_z}$ the oscillator length) is the classical radius of the free gas in the z-direction, and a_s is the s-wave scattering length for the two-body interactions. The system is then described by the effective 1D
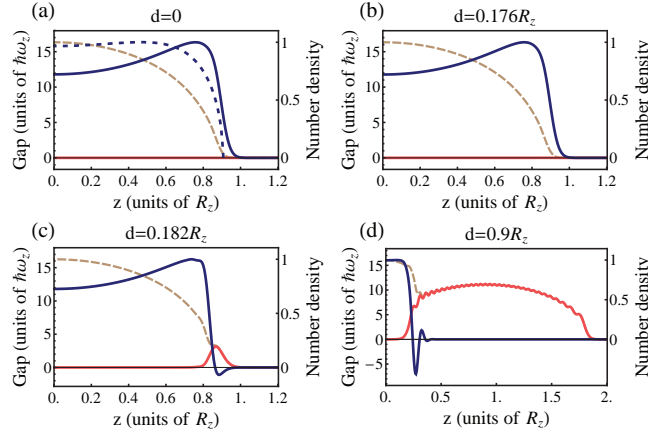
FIG. 3: (Color Online)(a-d) Spatial profile of the gap, total density, and magnetization in the $z \geq 0$ region (represented as in Fig. 1(b)) at $d = 0$, 0.176, 0.182, and $0.9R_z$, respectively. In addition, in (a), the gap function obtained by BCS plus LDA is shown (dashed blue curve). In (b) and (c), the separations are just below and above the critical value d_c for appearance of the first node. Note the scale change on the z-axis in (d).
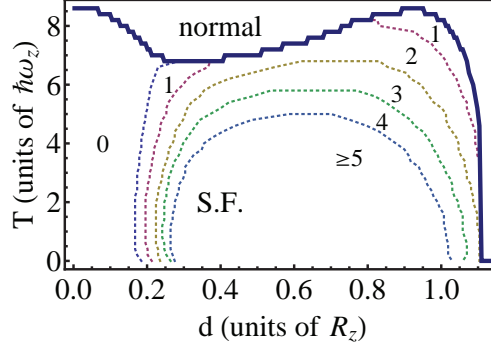

FIG. 4: (Color Online)Phase diagram as a function of separation and temperature ($N = 40$, $g/\hbar\omega_z R_z = 1$). The solid line separates the normal phase and the superfluid phase. In the superfluid phase, the dashed lines separate regions of the gap functions with different number of nodes.

Hamiltonian,

$$H = \int dz \big(\sum_\sigma \hat{\psi}_\sigma^\dagger H_\sigma^0 \hat{\psi}_\sigma + g \hat{\psi}_\uparrow^\dagger \hat{\psi}_\downarrow^\dagger \hat{\psi}_\downarrow \hat{\psi}_\uparrow \big), \tag{2}$$

where $H_\sigma^0 = -(\hbar^2/2m)\partial_z^2 + V_\sigma(z) - \mu_0$ is the one-particle Hamiltonian. The 1D coupling constant is given as $g = 2\hbar^2 a_{\rm s}/[m\ell_r^2(1 - 1.033 a_{\rm s}/\ell_r)]$ with the transverse oscillator length $\ell_r = \sqrt{\hbar/m\omega_r}$ [23].

We analyze our system within the standard BdG treatment, which has been widely applied to the imbalanced system [24], taking into account spin-dependent trapping. The mean-field Hamiltonian, which self-consistently incorporates the Hartree potential $U_\sigma = g\langle\hat{\psi}_\sigma^\dagger\hat{\psi}_\sigma\rangle$ and pairing gap $\Delta = g\langle\hat{\psi}_\downarrow\hat{\psi}_\uparrow\rangle$, takes the form

$$H_M = \int dz \big[\sum_\sigma \hat{\psi}_\sigma^\dagger(H_\sigma^0 + U_\sigma)\hat{\psi}_\sigma + (\Delta\hat{\psi}_\uparrow^\dagger\hat{\psi}_\downarrow^\dagger + {\rm h.c.}) \big]. \tag{3}$$

We obtain the extended BdG equations in the quasi-particle eigenbasis by a spin-dependent Bogoliubov transformation, $\hat{\psi}_\sigma(z) = \sum_n [u_{n\sigma}(z)\hat{\gamma}_{n\sigma} - \sigma v_{n\sigma}^*(z)\hat{\gamma}_{n,-\sigma}^\dagger]$. We use an iterative numerical procedure [25] to find self-consistent solutions for $\rho_\sigma(z)$ and $\Delta(z)$. Parity symmetry between the potentials of the two species, $V_\downarrow(z) = V_\uparrow(-z)$, ensures parity symmetry of the gap function; we find that the even-parity solution, $\Delta(z) = \Delta(-z)$, is always energetically favorable. The data presented in the following were obtained for $N = 40$ and $g/\hbar\omega_z R_z = 1$.

We first focus on the manner in which oscillatory pairing correlations emerge with increasing separation d. In Fig. 3, we show the pairing gap $\Delta(z)$, total density $\rho(z)$, and magnetization $M(z)$ for a sequence of four spin-split-trap systems with increasing d. Panel (a) shows the $d = 0$ case which is fully paired with $M = 0$ everywhere, as expected. The non-monotonicity of $\Delta(z)$ roughly reflects the functional dependence of the 1D BCS gap on the local
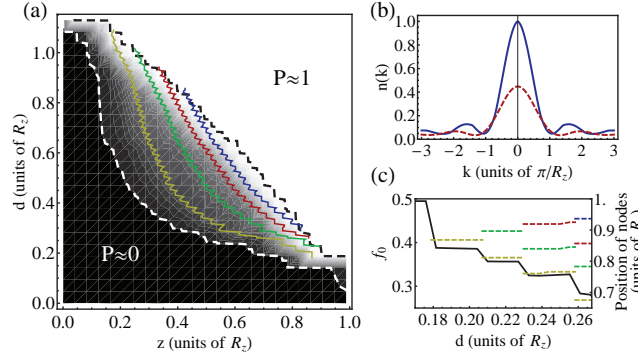
FIG. 5: (Color Online)(a) Density plot of the polarization P as a function of position z and separation d. The gray scale is bounded by 0 and 1. The dashed white (black) contours correspond to $P = 0.01$ (0.99). The solid curves indicate positions of the first four nodes. (b) Momentum distribution $n(k)$ for $d = 0$ (solid blue curve) and $0.25R_z$ (dashed red curve), normalized by $n(0)$ at $d = 0$. (c) Fraction of pairs f_0 within the central peak (see (b)) of $n(k)$ (solid curve, axis on left-hand side of graph) and positions of the first four nodes (dashed curves, axis on right-hand side of graph) vs d.

chemical potential μ, i.e., $\Delta(z) \propto \mu(z) \exp[-\sqrt{2\hbar^2 \pi^2 \mu(z)/(mg^2)}]$. Panel (b) shows that a small separation, $d < d_c$, does not lead to qualitative changes of the pairing correlations and the magnetization. Here, the local h is small enough everywhere that it is energetically favorable for the system to remain fully paired (i.e., the system is below the Clogston limit). Panel (c) shows the system just beyond the critical separation d_c, such that, near the edge of the cloud where the local h is largest and of order Δ, the gap function $\Delta(z)$ exhibits a node and the magnetization is finite. As d increases further, the region of oscillatory FFLO correlations increases and more nodes appear. The progression of nodes is captured in Figs. 1(b) and 3(c,d). Initially the number of nodes increases as d increases, but then, beyond a characteristic distance of the order of the cloud size, diminishes before the system fully separates and becomes normal.

We find that the nodal structure is robust against finite temperature effects. This is illustrated in the global phase diagram in Fig. 4, obtained using the parameter values specified above. Within the superfluid phase, regions with different numbers of nodes in $\Delta(z)$ are indicated. We note that the transition temperature in the spatially modulated phase is of the same order as in the fully paired phase. The number of nodes decreases with increase in temperature, consistent with the shrinking of the FFLO region in globally imbalanced systems [26]. As for trends with variation of the system parameters, we numerically find that the critical separation $\tilde{d}_c = d_c/R_z$ is independent of N and linearly dependent on $\tilde{g} = g/(\hbar\omega_z R_z)$ around $\tilde{g} = 1$ (in the regime of numerical convergence), which is consistent with rough estimates based on BCS combined with LDA.

Our results for the behavior of interacting fermions in the spin-split trap clearly show the intimate connection between a nonzero polarization and oscillatory pairing correlations. In Fig. 5(a) we show the polarization, $P(z) = M(z)/\rho(z)$, as a function of position, z, and separation, d, along with the spatial position of the nodes in $\Delta(z)$. It can be seen that the nodes only exist in the partially-polarized region, $0 < P < 1$. The correlation between the polarization and nodal structure indicates that this region is indeed of the FFLO type, and is surrounded by a fully gapped superfluid for $P \to 0$ towards the center of the spin-split trap and a fully polarized normal fluid for $P \to 1$ at the edges.

A direct measure of oscillatory pairing is the pair momentum distribution function defined as

$$n(k) = \int dz\, dz' e^{ik(z-z')} \langle \hat{\psi}_\uparrow^\dagger(z) \hat{\psi}_\downarrow^\dagger(z) \hat{\psi}_\downarrow(z') \hat{\psi}_\uparrow(z') \rangle, \tag{4}$$

which is experimentally measurable in dynamic-projection experiments [27]. In the homogeneous case, the FFLO phase is characterized by a peak in $n(k)$ at a characteristic nonzero wavevector k that depends on the spin-imbalance [11, 12]. Typical plots of $n(k)$ in the spin-split trap are shown in Fig. 5(b) for the cases of $d = 0$ and $d > d_c$. Due to the spatial inhomogeneity of the potential imbalance h, the system does not possess a characteristic wavevector. However, $n(k)$ undergoes sudden changes with increasing separation as Cooper pairs are shifted to higher momenta. As shown in Fig. 5(c), the weight under the central peak suddenly decreases each time a new node appears in $\Delta(z)$. Thus, $n(k)$ displays a striking signature of the modulated phase.

We now turn to the issue of experimentally realizing a spin-split-trap system. This setup can be achieved via spin-selective trapping potentials [28, 29]. Additionally, a tunable spin-split trap may be achieved using a magnetic field gradient [22, 30, 31], exploiting the distinct hyperfine-Zeeman states of the two fermion species. To see this, we note that the competition between the Zeeman effect and hyperfine interaction leads to a nonlinear energy difference

between the two spin states $m_{F\pm}$. We use the Breit-Rabi formula [32] to find the spatially-varying part of the energy difference $\Delta V(z) = V_\uparrow(z) - V_\downarrow(z)$ in the presence of a field gradient. Assuming a spatially-varying field of the form $B(z) = \bar{B} + B'z$ and expanding the Breit-Rabi formula near the background field $\bar{B}$, we obtain $\Delta V(z) = 2\pi\hbar B'\tilde{\mu}(\bar{B})z$ with $\tilde{\mu}$ the effective "magnetic moment" given by

$$\tilde{\mu}(\bar{B}) = \frac{g}{2}\mu_B \sum_{\sigma=\pm} \sigma \frac{\frac{2m_{F\sigma}}{2I+1} + \frac{\bar{B}}{B_0}}{\sqrt{1 + \frac{4m_{F\sigma}}{2I+1}\frac{\bar{B}}{B_0} + \frac{\bar{B}^2}{B_0^2}}}. \tag{5}$$

Here, μ_B is the Bohr magneton, I is the nuclear spin, B_0 is the hyperfine field, and $g \simeq 2$.

Using Eq. (1), we see that a spatial separation d requires a field gradient $B' = 2m\omega_z^2 d/\tilde{\mu}$. In the case of interest, we expect that $\bar{B}$ is close to a Feshbach resonance (FR) in order to enhance T_c, and that B' is small enough that a_s can be treated spatially independent in the system. For ^{6}Li ($I = 1$, $B_0 = 81$G), using the hyperfine levels $m_{F\pm} = -\frac{3}{2}(+\frac{1}{2})$ [33] near the FR at $\bar{B} = 691$G, we find $\tilde{\mu}_{Li} \simeq 6 \times 10^{-3}\mu_B$. Assuming a typical trap frequency $\omega_z \sim 2\pi \times 100$Hz, a field gradient B'_{Li} of the order of a few 100G/cm can achieve a separation d of a few ℓ_z. (The required field gradient for the more commonly used two lowest hyperfine levels of ^{6}Li is about an order of magnitude larger and, thus, much less experimentally viable.) The most promising case is that of ^{40}K ($I = 4$, $B_0 = -459$G) with $m_{F\pm} = -\frac{7}{2}(-\frac{9}{2})$ near the FR at $\bar{B} = 202$G. Here $\tilde{\mu}_K \simeq 0.1\mu_B$ and, for the same ω_z as above, the required gradient $B'_K \simeq 50$G/cm.

In summary, we have proposed a novel setting, the spin-split trap, for observing FFLO-like oscillatory pairing correlations, driven by a local density imbalance due to the separate trapping potentials of the two fermion species. Our BdG calculations, supported by LDA, show that the competition between the tendency to pair and the tendency towards forming a spin imbalance leads to a rich structure that is revealed in quantities such as the local pairing amplitude and magnetization, as well as in the pair momentum distribution. Immediate future directions include investigating the spin-split system through other techniques amenable to 1D, such as DMRG and quantum Monte Carlo methods, and exploring the exciting prospect of coupling arrays of spin-split 1D systems.

[1] P. Fulde and R.A. Ferrell, Phys. Rev. **135**, A550 (1964).
[2] A.I. Larkin and Yu.N. Ovchinnikov, Zh. Eksp. Teor. Fiz **47**, 1136 (1964) [Sov. Phys. JETP **20**, 762 (1965)].
[3] See, e.g., A.I. Buzdin, Rev. Mod. Phys. **77**, 935 (2005).
[4] I. Bloch, J. Dalibard, and W. Zwerger, Rev. Mod. Phys. **80**, 885 (2008).
[5] S. Giorgini, L.P. Pitaevskii, and S. Stringari, Rev. Mod. Phys. **80**, 1215 (2008).
[6] W. Ketterle and M. Zwierlein, preprint arXiv:0801.2500 (2008).
[7] For review see L. Radzihovsky and D.E. Sheehy, Rep. Prog. Phys. **73**, 076501 (2010).
[8] K. Yang, Phys. Rev. B **63**, 140511(R) (2001).
[9] G. Orso, Phys. Rev. Lett. **98**, 070402 (2007).
[10] H. Hu, X.-J. Liu, and P.D. Drummond, Phys. Rev. Lett. **98**, 070403 (2007).
[11] A.E. Feiguin and F. Heidrich-Meisner, Phys. Rev. B **76**, 220508(R) (2007).
[12] G.G. Batrouni et al, Phys. Rev. Lett. **100**, 116405 (2008).
[13] E. Zhao and W.V. Liu, Phys. Rev. A **78**, 063605 (2008).
[14] G. Orso, E. Burovski, and T. Jolicoeur, Phys. Rev. Lett. **104**, 065301 (2010).
[15] A-H. Chen and X. Gao, Phys. Rev. A **81**, 013628 (2010).
[16] I. Zapata et al, Phys. Rev. Lett. **105**, 095301 (2010).
[17] D.E. Sheehy and L. Radzihovsky, Phys. Rev. Lett. **96**, 060401 (2006); Ann. of Phys. **322**, 1790 (2007).
[18] M.M. Parish et al, Nat. Phys. **3**, 124 (2007).
[19] N. Yoshida and S.-K. Yip, Phys. Rev. A **75**, 063601 (2007).
[20] Y. Liao et al, Nature **467**, 567 (2010).
[21] A. Recati et al, Phys. Rev. Lett. **97**, 190403 (2006).
[22] H. Moritz et al, Phys. Rev. Lett. **94**, 210401 (2005).
[23] M. Olshanii, Phys. Rev. Lett. **81**, 938 (1998).
[24] T. Mizushima, K. Machida, and M. Ichioka, Phys. Rev. Lett. **94**, 060404 (2005); J. Kinnunen, L.M. Jensen, and P. Törmä, Phys. Rev. Lett. **96**, 110403 (2006).
[25] R.A. Riedel, L.-F. Chang, and P.F. Bagwell, Phys. Rev. B **54**, 16082 (1996).
[26] M.J. Wolak et al, Phys. Rev. A **82**, 013614 (2010).
[27] C.A. Regal, M. Greiner, and D.S. Jin, Phys. Rev. Lett. **92**, 040403 (2004); E. Altman and A. Vishwanath, Phys. Rev. Lett. **95**, 110404 (2005).

[28] J. Catani et al, Phys. Rev. Lett. **103**, 140401 (2009).
[29] D. McKay and B. DeMarco, New J. Phys. **12**, 055013 (2010).
[30] D.M. Weld et al, Phys. Rev. Lett. **103**, 245301 (2009).
[31] K. Jiménez-García et al, Phys. Rev. Lett. **105**, 110401 (2010).
[32] G. Breit and I.I. Rabi, Phys. Rev. **38**, 2082 (1931).
[33] C.H. Schunck et al, Nature **454**, 739 (2008).